CMST 29(1–4) 57–64 (2023) DOI:10.12921/cmst.2023.0000027

Density Functional Formalism as a Description of the Elastic Behavior of a Hard-Sphere Crystal

S. Pieprzyk[1*], **A.C. Brańka**[1†], **D.M. Heyes**[2]

[1] *Institute of Molecular Physics*
Polish Academy of Sciences
M. Smoluchowskiego 17, 60-179 Poznań, Poland
[*] *E-mail: slawomir.pieprzyk@ifmpan.poznan.pl*
[†] *E-mail: branka@ifmpan.poznan.pl*

[2] *Royal Holloway, University of London*
Department of Physics
Egham, Surrey TW20 0EX, United Kingdom
E-mail: david.heyes@rhul.ac.uk

Received: 13 November 2023; in final form: 20 November 2023; accepted: 21 November 2023; published online: 9 December 2023

Abstract: The density functional method of Jarić and Mohanty [Phys. Rev. B **37**, 4441 (1988)] for calculating the elastic moduli of crystalline solids is considered here from the perspective of some new findings. The very slow convergence of the reciprocal-lattice vector summations and presence of the three body term in the method's computational scheme identified in [J. Chem. Phys. **118**, 6594 (2003)] is confirmed and discussed. The sensitivity of the results to the scheme parameters, such as the width of the Gaussian density profiles and the Percus-Yevick approximation used for the direct correlation function is explored. The calculations are for a hard-sphere crystal but most conclusions can be applicable to model crystalline solids in general.

Key words: density functional theory, elastic moduli tensor, hard spheres

I. Introduction

Density functional theory (DFT) has been widely used in condensed matter, computational physics and chemistry quantum applications. The application of DFT used in this work is the classical analog of the popular methods of Hohenberg and Kohn [1] and Kohn and Sham [2, 3]. The theoretical basis of this classical DFT version is a theorem by Mermin [4] which establishes a one-to-one correspondence between the local density and the external potential. This allows us to express the thermodynamic potential of a system (e.g., the Helmholtz or Gibbs free energy) as a functional of the local density [5]. The DFT method has probably found its greatest application in the study of first-order phase transitions, in particular in the description and prediction of freezing [6–10].

The hard-sphere (HS) system has been the standard test of DFT methods of freezing and their development. The advantage of using the HS system is that its phase diagram only depends on the density, and the Percus-Yevick (PY) equation [11] gives a fairly accurate approximation of the two-particle direct correlation function (DCF) used in the theory.

Several forms of DFT have been developed [11–16] and in the context of the freezing-melting transition investigations the approach based on a thermodynamic perturbation expansion around a liquid state has often been exploited. This was formulated in the language of the direct correlation function by Ramakrishnan and Yussouff (RY) [9, 17, 18].

Tab. 1. List of acronyms used in this work and their explanations

Acronym	Explanation
DFT	density functional theory
HS	hard-sphere
MD	molecular dynamics
MC	Monte Carlo
PR	Poisson's ratio
DCF	direct correlation function
PY	Percus-Yevick
RFA	rational function approximation
RY	Ramakrishnan and Yussouff
JM	Jarić and Mohanty
BC	Baus and Colot
FL	Frenkel and Ladd
TW	Tretiakov and Wojciechowski
SSM	Sushko, van der Schoot and Michels

Within the framework of the RY approach the first DFT application for calculating elastic constants of crystalline solids was proposed by Jarić and Mohanty (JM) [19–21]. In their approach the distribution of particle positions in a crystal, as expressed in terms of the one particle distribution function, are represented by the summation of narrow Gaussians, and the crystal is related to a chosen reference liquid. It should be mentioned that the results obtained from these DFT calculations have been considered to be largely unsatisfactory. First, the elastic constants obtained differed significantly from those determined by computer simulations, e.g., the difference for the shear elastic component at the melting was more than three hundred percent [21]. Secondly, the authors obtained a negative Poisson's ratio (PR) for hard-spheres which is qualitatively incorrect, as was pointed out by Frenkel and Ladd [22]. In reply, Jarić and Mohanty [23] suggested that the inclusion of the three-body direct correlation function could improve the results. Their conclusion was that by the inclusion of the main part of the three-body direct correlation function [24] a positive value for the PR can be achieved but, as was shown, its magnitude was far too low.

In 2003, Sushko *et al.* [25] demonstrated that the proposed three-body correction term is indeed significant and it is possible to improve the original theory by adding this extra term. These authors showed that the values of the elastic constants can depend significantly on the number of reciprocal-lattice vectors used in the calculations, which were not sufficient in the calculations of Jarić and Mohanty. Therefore, it may be concluded that Sushko *et al.* found that the DFT approach can provide reasonable agreement with the computer simulations, when the three-body direct correlation function and enough number of reciprocal-lattice vectors are included in the summation.

Taking into account the significance of these findings and that there are more recent computer simulation values for the elastic constants of the hard-sphere crystal in the literature, we have revisited the density functional route in this work. The DFT approach used to calculate the elastic properties here is presented in the next section, Sec. II. In Sec. III, the role of the number of reciprocal-lattice vectors employed in the calculation scheme is discussed in more detail. Also, in that section the robustness of the results to the model parameters and the significance of the approximation used for the DCF are analyzed. Conclusions are made in Sec. IV. A list of the acronyms used in this work is given in Tab. 1.

II. Elastic Constants from the DFT

The main aim of this section is to present how the elastic constants of the HS crystal are expressed in terms of the DFT elastic components. As the thermodynamically stable structure of the HS crystal is considered to be face-centered cubic (fcc) the expressions presented below are for cubic symmetry (the more general formulas are given in the original JM work [21]).

A one-particle density distribution $\rho(\mathbf{r})$ in the crystalline phase can be approximated well by a lattice sum of narrow Gaussians with the same variance,

$$\rho(\mathbf{r}) = \frac{\rho_{\mathrm{S}}}{N_{\mathrm{c}}\pi^{3/2}\alpha^{3/2}} \sum_{\{\mathbf{R}\}} \exp\left(-\frac{(\mathbf{R}-\mathbf{r})^2}{a^2\alpha}\right), \qquad (1)$$

where $\mathbf{R}$ indicates the set of the real-space perfect crystal lattice vectors, $\mathbf{r}$ is the instantaneous position of the particle, a is the lattice constant, α describes the (dimensionless) width of the Gaussian local density profile (measured in units of the lattice constant a), $\rho_{\mathrm{S}} = N_{\mathrm{c}}/a^3$ is the average density of the crystal, and N_{c} is the number of sites per unit cell.

In the method proposed by JM the elastic free energy of the strained solid is expanded around the unstrained state in terms of the strain ϵ and α variation [21]. The isothermal elastic moduli are computed from the quadratic terms (the zero- and first-order terms vanish [21]) by first minimizing the grand thermodynamic potential of the unstrained solid [10, 25],

$$\begin{aligned}\Delta\omega \;=\; & 1-(1+\eta)\left(\frac{5}{2}+ln\frac{N_{\mathrm{c}}\pi^{3/2}\alpha^{3/2}}{1+\eta}+\right. \qquad (2)\\ & \left.+\frac{1}{k_{\mathrm{B}}T}(\mu_{\mathrm{S}}-\mu_{\mathrm{L}})\right)-\frac{1}{2}\eta^2\rho_{\mathrm{L}}c_{\mathrm{L}}^{(2)}(0)+\\ & -\frac{1}{2}\rho_{\mathrm{L}}\sum_{\{\mathbf{G}\}}\xi_{\mathrm{G}}^2 c_{\mathrm{L}}^{(2)}(|\mathbf{G}|)-\frac{1}{6}\eta^3\rho_{\mathrm{L}}^2 c_{\mathrm{L}}^{(3)}(0,0),\end{aligned}$$

with respect to the density of the reference liquid ρ_{L}, the equilibrium width α and the lattice constant parameter a (from which the solid density, ρ_{S}, can be obtained). In the above equation $\mathbf{G}$ is the set of the reciprocal-lattice wave vectors, $\eta = (\rho_{\mathrm{S}}-\rho_{\mathrm{L}})/\rho_{\mathrm{L}}$, k_{B} is the Boltzmann constant, T is the temperature, μ_{S} and μ_{L} are the chemical potentials of solid and liquid phase, respectively. The second minimization is with respect to the variational parameter $\Delta\alpha = \alpha(\epsilon) - \alpha$.

From the minimizing procedure the following elastic modulus tensor was obtained [21],

$$\mathbf{C} = \mathbf{C}^{\epsilon\epsilon} - \mathbf{C}^{\epsilon\alpha} : (\mathbf{C}^{\alpha\alpha})^{-1} : \mathbf{C}^{\alpha\epsilon}. \tag{3}$$

For cubic crystals there are three independent elastic constants which in Voigt notation are denoted by C_{11}, C_{12} and C_{44} [26].

The resultant expressions for the elastic moduli components of cubic solid in the DFT formulation are [21, 25],

$$\begin{aligned}\tilde{C}^{\epsilon\epsilon}_{11} &= (\eta+1) - (\eta+1)^2\rho_{\mathrm{L}}c^{(2)}_{\mathrm{L}}(0) + \\ &-\rho_{\mathrm{L}}\sum_{\{\mathbf{G}\}}\xi^2_{\mathrm{G}}c^{(2)}_{\mathrm{L}}(|\mathbf{G}|) - \eta(\eta+1)^2\rho^2_{\mathrm{L}}c^{(3)}_{\mathrm{L}}(0,0) + \\ &-\frac{1}{2}\rho_{\mathrm{L}}\sum_{\{\mathbf{G}\}}\xi^2_{\mathrm{G}}\left(\frac{c^{''(2)}_{\mathrm{L}}(|\mathbf{G}|)}{|\mathbf{G}|^2} - \frac{c^{'(2)}_{\mathrm{L}}(|\mathbf{G}|)}{|\mathbf{G}|^3}\right)G_1^4, \end{aligned} \tag{4a}$$

$$\tilde{C}^{\epsilon\alpha}_{11} = -\frac{\eta+1}{2\alpha} - \frac{a^2}{4}\rho_{\mathrm{L}}\sum_{\{\mathbf{G}\}}\xi^2_{\mathrm{G}}\frac{c^{'(2)}_{\mathrm{L}}(|\mathbf{G}|)}{|\mathbf{G}|}G_1^4, \tag{4b}$$

$$\tilde{C}^{\alpha\alpha}_{11} = \frac{\eta+1}{2\alpha^2} - \frac{a^4}{8}\rho_{\mathrm{L}}\sum_{\{\mathbf{G}\}}\xi^2_{\mathrm{G}}c^{(2)}_{\mathrm{L}}(|\mathbf{G}|)G_1^4, \tag{4c}$$

$$\begin{aligned}\tilde{C}^{\epsilon\epsilon}_{12} &= (\eta+1) - (\eta+1)^2\rho_{\mathrm{L}}c^{(2)}_{\mathrm{L}}(0) + \\ &-\rho_{\mathrm{L}}\sum_{\{\mathbf{G}\}}\xi^2_{\mathrm{G}}c^{(2)}_{\mathrm{L}}(|\mathbf{G}|) - \eta(\eta+1)^2\rho^2_{\mathrm{L}}c^{(3)}_{\mathrm{L}}(0,0) + \\ &-\frac{1}{2}\rho_{\mathrm{L}}\sum_{\{\mathbf{G}\}}\xi^2_{\mathrm{G}}\left(\frac{c^{''(2)}_{\mathrm{L}}(|\mathbf{G}|)}{|\mathbf{G}|^2} - \frac{c^{'(2)}_{\mathrm{L}}(|\mathbf{G}|)}{|\mathbf{G}|^3}\right)G_1^2G_2^2, \end{aligned} \tag{4d}$$

$$\tilde{C}^{\epsilon\alpha}_{12} = -\frac{\eta+1}{2\alpha} - \frac{a^2}{4}\rho_{\mathrm{L}}\sum_{\{\mathbf{G}\}}\xi^2_{\mathrm{G}}\frac{c^{'(2)}_{\mathrm{L}}(|\mathbf{G}|)}{|\mathbf{G}|}G_1^2G_2^2, \tag{4e}$$

$$\tilde{C}^{\alpha\alpha}_{12} = -\frac{a^4}{8}\rho_{\mathrm{L}}\sum_{\{\mathbf{G}\}}\xi^2_{\mathrm{G}}c^{(2)}_{\mathrm{L}}(|\mathbf{G}|)G_1^2G_2^2, \tag{4f}$$

$$\tilde{C}^{\epsilon\epsilon}_{44} = -\frac{1}{2}\rho_{\mathrm{L}}\sum_{\{\mathbf{G}\}}\xi^2_{\mathrm{G}}\left(\frac{c^{''(2)}_{\mathrm{L}}(|\mathbf{G}|)}{|\mathbf{G}|^2} - \frac{c^{'(2)}_{\mathrm{L}}(|\mathbf{G}|)}{|\mathbf{G}|^3}\right)G_1^2G_2^2, \tag{4g}$$

$$\tilde{C}^{\epsilon\alpha}_{44} = -\frac{a^2}{4}\rho_{\mathrm{L}}\sum_{\{\mathbf{G}\}}\xi^2_{\mathrm{G}}\frac{c^{'(2)}_{\mathrm{L}}(|\mathbf{G}|)}{|\mathbf{G}|}G_1^2G_2^2, \tag{4h}$$

$$\tilde{C}^{\alpha\alpha}_{44} = \frac{\eta+1}{4\alpha^2} - \frac{a^4}{8}\rho_{\mathrm{L}}\sum_{\{\mathbf{G}\}}\xi^2_{\mathrm{G}}c^{(2)}_{\mathrm{L}}(|\mathbf{G}|)G_1^2G_2^2. \tag{4i}$$

In the above expressions $c^{(2)}_{\mathrm{L}}(|\mathbf{G}|)$ is the liquid direct correlation function, and $c^{'(2)}_{\mathrm{L}}(|\mathbf{G}|)$, $c^{''(2)}_{\mathrm{L}}(|\mathbf{G}|)$ are their first and second derivatives.

In the equations,

$$\xi_{\mathrm{G}} = (\eta+1)\exp\left(-\frac{1}{4}|\mathbf{G}|^2a^2\alpha\right), \tag{5}$$

which is basically a Fourier representation of the Gaussian density distribution in Eq. (1), and the DFT elastic coefficients are in the dimensionless form $\tilde{C}_{ij} = C_{ij}/k_{\mathrm{B}}T\rho_{\mathrm{L}}$.

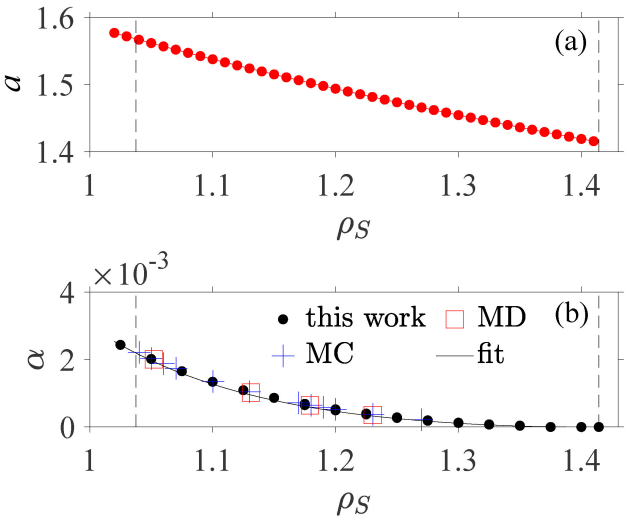

Fig. 1. In frame (a) the lattice constant a is shown as a function of the solid density, ρ_{S}. In frame (b) the α parameter (measured in units of the lattice constant a) which describes the (dimensionless) width of the one-particle density profile is shown as a function of solid density. The solid black points represent the MD data obtained in this work. The solid black line is a 4th order polynomial fit to the data. The blue pluses and red open squares are data from Ref. 27 and 28, respectively. The vertical thin dashed lines indicate the melting and close packing densities

Note that the three-body direct correlation function term is present in the above equations (2), (4a) and (4d). Sushko *et al.* [10, 25] used the three-body DCF terms proposed by [23], as an advance on their original formulation [21]. The three-body term can be calculated as the density derivative of $c^{(2)}_{\mathrm{L}}(q)$ [10, 25],

$$c^{(3)}_{\mathrm{L}}(q,0) = \left.\frac{\partial c^{(2)}_{\mathrm{L}}(q)}{\partial\rho}\right|_{\rho=\rho_{\mathrm{L}}}. \tag{6}$$

To compute the above elastic moduli from the expressions in Eqs. (4) the values of α, ρ_{S} and ρ_{L} are needed. In the JM method these quantities are obtained as the result of the minimization of Eq. (2) for the unstrained solid i.e., from the first minimization.

Finally, the elastic constants of the HS crystal according Eqs. (3) and (4) are (see Appendix C in Ref. 21),

$$\tilde{C}_{11} = \tilde{C}^{\epsilon\epsilon}_{11} - \frac{1}{3}\frac{\left(\tilde{C}^{\epsilon\alpha}_{11}+2\tilde{C}^{\epsilon\alpha}_{12}\right)^2}{\tilde{C}^{\alpha\alpha}_{11}+2\tilde{C}^{\alpha\alpha}_{12}} - \frac{2}{3}\frac{\left(\tilde{C}^{\epsilon\alpha}_{11}-\tilde{C}^{\epsilon\alpha}_{12}\right)^2}{\tilde{C}^{\alpha\alpha}_{11}-\tilde{C}^{\alpha\alpha}_{12}}, \tag{7a}$$

$$\tilde{C}_{12} = \tilde{C}^{\epsilon\epsilon}_{12} - \frac{1}{3}\frac{\left(\tilde{C}^{\epsilon\alpha}_{11}+2\tilde{C}^{\epsilon\alpha}_{12}\right)^2}{\tilde{C}^{\alpha\alpha}_{11}+2\tilde{C}^{\alpha\alpha}_{12}} + \frac{1}{3}\frac{\left(\tilde{C}^{\epsilon\alpha}_{11}-\tilde{C}^{\epsilon\alpha}_{12}\right)^2}{\tilde{C}^{\alpha\alpha}_{11}-\tilde{C}^{\alpha\alpha}_{12}}, \tag{7b}$$

$$\tilde{C}_{44} = \tilde{C}^{\epsilon\epsilon}_{44} - \frac{\left(\tilde{C}^{\epsilon\alpha}_{44}\right)^2}{\tilde{C}^{\alpha\alpha}_{44}}. \tag{7c}$$

To analyze the above expressions for the DFT approach, there are several issues to be considered. First, the influence of the $c_{\mathrm{L}}^{(3)}(0,0)$ term on the $\tilde{C}_{ij}$ values and other elastic properties such as the PR has to be verified. This issue was investigated and, as mentioned in the Introduction, the three-body term was observed previously to improve the level of agreement of the elastic constants with those obtained directly by computer simulation [23, 25]. Secondly, as indicated by Sushko *et al.* [25] the results obtained with Eqs. (4) can be quite sensitive to the number of the reciprocal wave vectors $\mathbf{G}$ used in the summations, and in fact it was shown that as many as 20 000 vectors are required to obtain $\tilde{C}_{ij}$ values that are sufficiently converged to make a meaningful comparison with the simulation values. This extremely slow convergence probably could not have been observed in calculations carried out in the 1980s with the computer resources available at that time.

The third issue is the type of approximation for the direct correlation function used in the calculations, which previously was using the Percus-Yevick analytic solution. Also, the first minimization procedure gives the values for α, a (or ρ_{S}) which only approximates the simulation values. All of these issues are explored in the next section.

III. Results

The Monte Carlo (MC) derived elastic properties by Tretiakov and Wojciechowski [29, 30] are used to compare with the DFT approximation predictions. The parameters α and the lattice constant a were calculated from MD simulations carried out here. The HS system consisted of $N = 4000$ particles in the simulation box which was first equilibrated for 10^7 collisions, and then production data were collected over the following 10^8 collisions. The values of α and a as a function of solid density are shown in Fig. 1.

As Sushko *et al.* showed [25], to improve the JM DFT approach it is important not only to include the three-body term, but also to take a sufficient number of reciprocal-lattice vectors, as is demonstrated in Fig. 2 for three different solid densities. The calculated quantities become saturated only at a very large number of vectors, n_{c}, which increases with density (e.g., $n_{\mathrm{c}} \approx 20\,000$ is required for $\rho_{\mathrm{S}} \approx 1.1$). If $n < n_{\mathrm{c}}$ there are large oscillations about the final value, and only taking the first several tens of $\mathbf{G}$ vectors can give a misleading impression of convergence, as seen for the cumulative averages in Fig. 3. It seems that this behavior can lead to a qualitatively incorrect value of PR if the three-body term is not included in the calculations and a sufficient number of vectors is not taken in the summations. As was demonstrated in [25] including the three-body term and using $n > n_{\mathrm{c}}$ in the summations improved the agreement between the DFT and simulation data for the elastic properties of the fcc hard-sphere solid. However, as shown in Fig. 4a the agreement is far from perfect and is only at the order of magnitude level, while the $\tilde{C}_{ij}$ values differ quite significantly from the 'exact' simulation result which can be seen by comparing the dashed and solid lines with the same color.

A possible reason for this discrepancy may be the approximate values of the parameters used. As mentioned above, to compute the elastic moduli in Eqs. (4) the α, ρ_{S} and ρ_{L} are determined from the minimization of $\Delta\omega$ in Eq. (2). The results of such an approach usually do not give

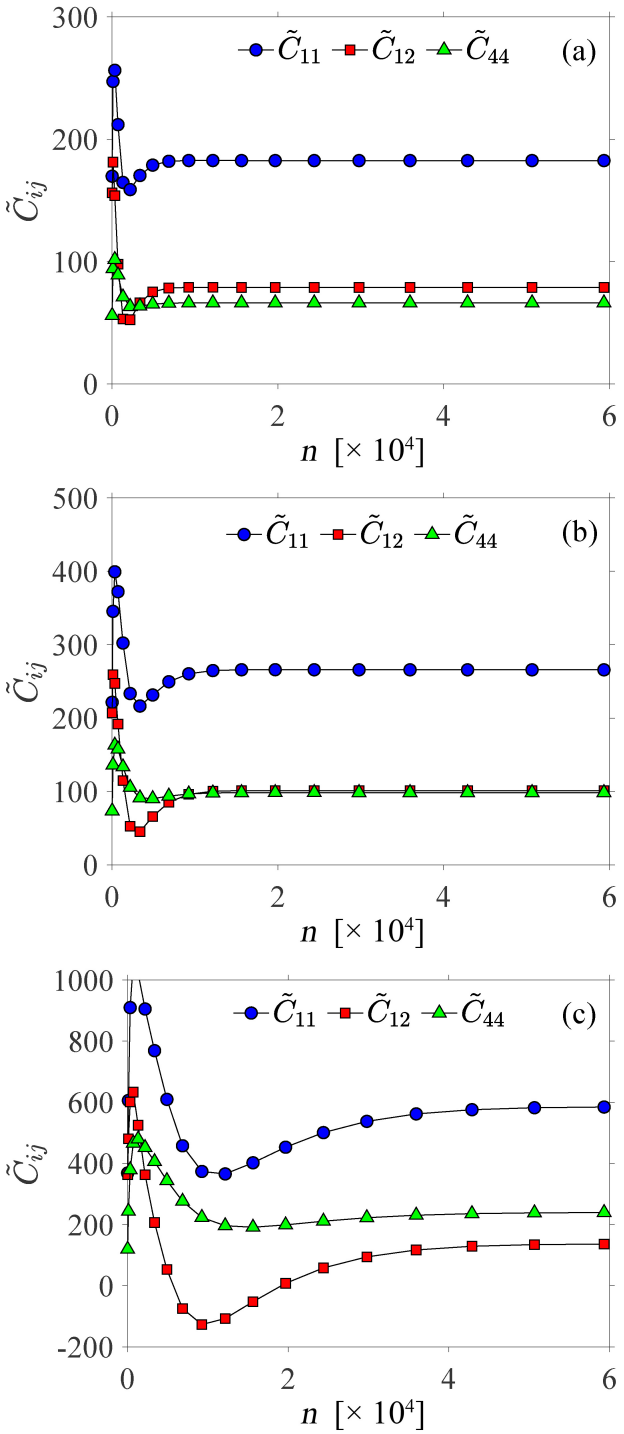

Fig. 2. The dependence of the dimensionless elastic moduli $\tilde{C}_{11}$ (blue points), $\tilde{C}_{12}$ (red squares), $\tilde{C}_{44}$ (green triangles) on the number, n, of the reciprocal-lattice vectors taken into account in the summation in Eqs. (4) is presented for the hard-sphere crystal at densities $\rho_{\mathrm{S}} = 1.05$ in frame (a), $\rho_{\mathrm{S}} = 1.10$ in (b) and $\rho_{\mathrm{S}} = 1.20$ in (c)

the values of $\alpha(\rho_S)$ and $a(\rho_S)$ from the MD simulations as presented in Fig. 1. The 'exact' HS crystal values for α and a from Fig. 1 were taken to check the behavior of Eqs. (4) (and therefore the expressions for $\tilde{C}_{ij}$ in Eqs. (7)) with variation of the input parameter values. With this assumption there are different possible schemes for establishing ρ_L and we considered one proposed by Baus and Colot (BC) [13, 14] in which the reference fluid is equal to the effective fluid defined in the DFT method. In their scheme the 'effective fluid density' is associated with the solid density for which the smallest value of the reciprocal-lattice vector G and the position of main peak of the static structure factor, $S(q)$ of the fluid overlap.

Using the BC approach the value of ρ_L was established for each of the crystal densities considered. The results of these calculations of the elastic constants are shown in Fig. 4a. As may be seen, the results from a different scheme for the parameter selection do not differ significantly from those previously obtained (represented by the dashed lines). The data points (closed symbols) still differ from the simulation data (the solid bold lines and open symbols) to a similar extent as obtained in Ref. 25. In Fig. 4b the Poisson's ratio along the [1,0,0] crystallographic direction, $\nu = (C_{12} + P)/(C_{11} + C_{12})$ is shown, where P is the pressure of the HS crystal calculated from the analytical Z_{S2} formula from Ref. 31. The DFT values are positive and follow quite well the simulation results, at least for the range of densities considered.

Finally, the influence of the PY approximation for the DCF, $c(q)$, is assessed by performing the calculations with the Rational Function Approximation (RFA) solution [32, 33]. The $c^{RFA}(r)$ function is considered to be a more accurate representation of the HS DCF in, for example, being non-zero for $r > \sigma$ [33]. The $c^{PY}(q)$ and calculated $c^{RFA}(q)$ (and their difference) from this study are shown in Fig. 5. As is visible, the main differences between these functions

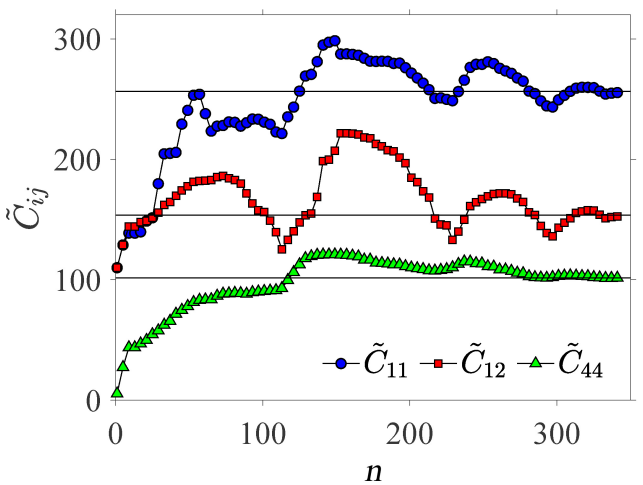

Fig. 3. The cumulative average of the dimensionless elastic moduli $\tilde{C}_{11}$ (blue points), $\tilde{C}_{12}$ (red squares) and $\tilde{C}_{44}$ (green triangles) as a function of the number, n, of reciprocal-lattice vectors used in the summation in Eqs. (4). The solid density, $\rho_S = 1.05$ and the solid horizontal lines are only to guide the eye

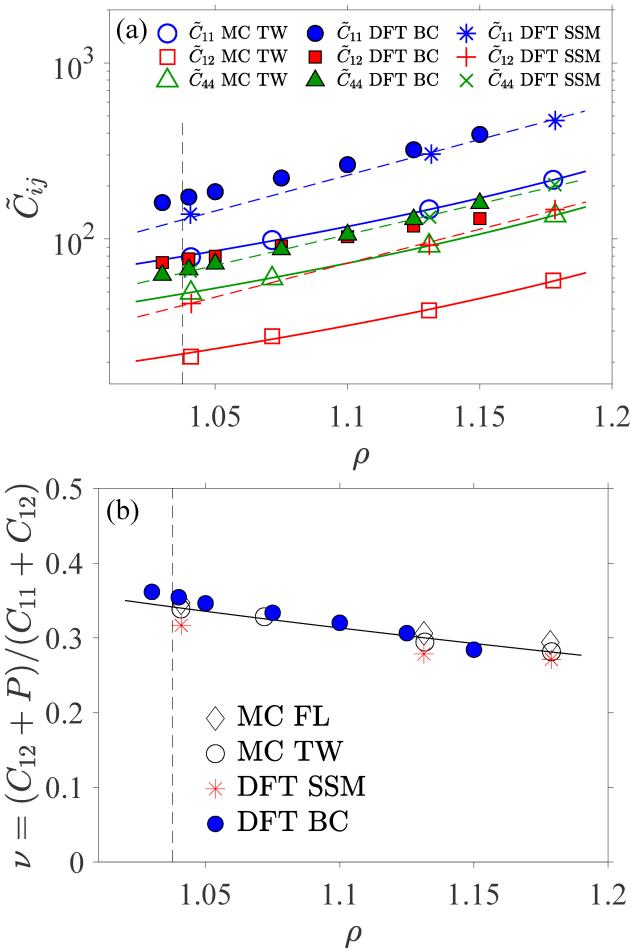

Fig. 4. In the top frame (a) the dimensionless elastic coefficients $\tilde{C}_{11}$, $\tilde{C}_{12}$ and $\tilde{C}_{44}$ are presented. In the bottom frame (b) the Poisson's ratio, ν is shown. In the figure: MC FL denotes Monte Carlo data by Frenkel and Ladd [22], MC TW are the Monte Carlo data by Tretiakov and Wojciechowski [29, 30], DFT SSM are the DFT results from Sushko *et al.* [25]. DFT BC denote results from this work (Eqs. (7) in Sec. III). The dashed and solid colored lines in frame (a) and the solid black line in frame (b) are to guide the eye. The vertical thin dashed lines in both frames indicate the melting density, $\rho_m = 1.0376$

are for $q < 10$, but a tiny oscillatory difference persists also for very large q. The $\tilde{C}_{ij}$ and PR values calculated with the RFA solution are given in Fig. 6. A comparison between Figs. 4 and 6 indicates that there is some influence on $c(q)$ from the approximation used in the DFT approach. The RFA approximation causes a relative reduction in the values of the coefficients obtained compared with the PY approximation. In particular, a very good representation of the $\tilde{C}_{44}$ coefficient is obtained. The slightly better agreement with the simulation data for $\tilde{C}_{11}$, $\tilde{C}_{12}$ and the good agreement for the PR at the melting density should be considered to be rather accidental.

IV. Summary and Concluding Remarks

The work concerns the problem of calculating elastic constants using the density functional theory. The issue of the

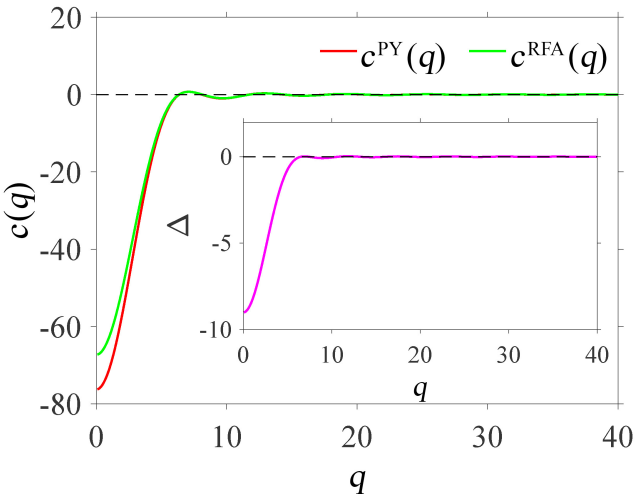

Fig. 5. The wave vector, q-dependence of the direct correlation function for a liquid density of $\rho_L = 0.9884$. The solid red and green lines represent the PY and RFA $c(q)$ data, respectively. The difference between these two approaches $\Delta = c^{PY}(q) + -c^{RFA}(q)$ is shown in the inset as a magenta line

convergence of the summations in the DFT method calculations is analyzed. The influence of varying some of the method's parameters and the approximate representation of the direct correlation functions are also assessed.

The importance of calculations with a sufficiently large number of reciprocal-lattice vectors was confirmed. Changes in the calculated elastic constants can be of the order of several hundred percent, depending on the minimum number of reciprocal vectors, n_c adopted. It is shown that the value of n_c to ensure sufficient convergence of the calculated sums increases significantly with density. Also, it is worth emphasizing that significant changes occur on a scale of several hundred reciprocal-lattice vectors $\mathbf{G}$, and therefore the true converged value can only be observed on the scale of several thousand $\mathbf{G}$ vectors.

The calculations indicate that small changes in the method's parameters a, α, and ρ_L do not affect significantly the calculated elastic constants $\tilde{C}_{ij}$. This means that variation of these parameters does not lead to a significant improvement in the consistency of the results obtained using DFT with the 'exact' simulation results.

The results of the DFT calculations with the rational function approximation solution slightly improve agreement of the elastic constants with the corresponding simulation derived quantities compared to the Percus-Yevick closure.

The calculations indicate that the use of an appropriate number of terms in the summations, the three-body term correction and a better approximation of the DCF may lead to a relatively good approximation for elastic constants and the Poisson's ratio, at least for the region close to the melting density, where the DFT method is expected to yield the best representation of the physical properties mainly because it is based on the density in the fluid phase.

Finally, note that the method considered in this work is not only intended for the HS system. It is a fairly general and fundamental approach which has also been proposed

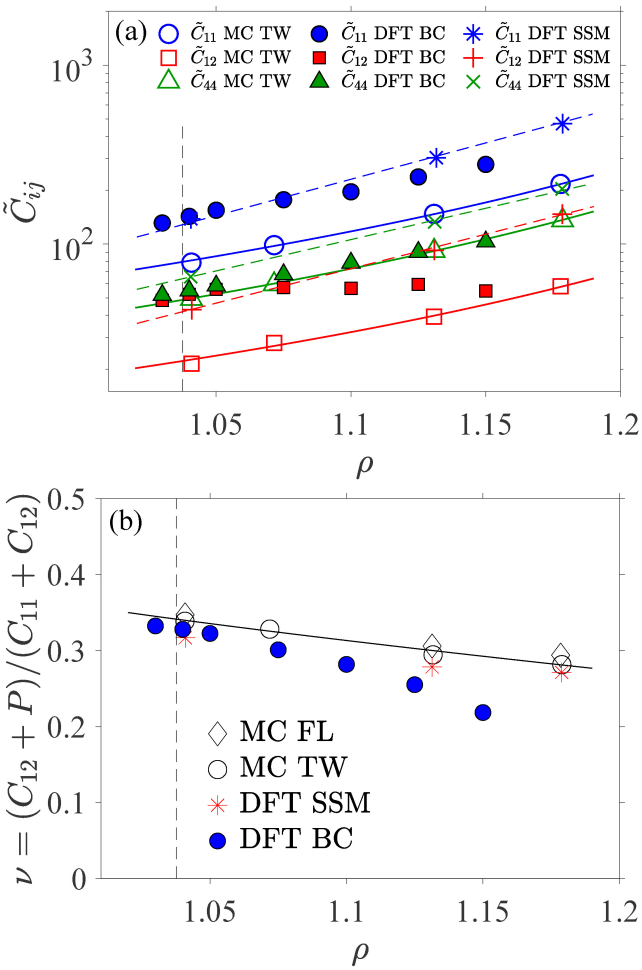

Fig. 6. As for Fig. 4 except that the PY solution was replaced by the RFA approach in the calculations

for other types of inter-particle interactions and solid symmetries. In fact, the authors who pointed out the key significance of the convergence of the sums in the calculation, applied it to the crystallization of the flexible polymeric chains [10, 25]. Also, the DFT elastic moduli are important ingredients of the revised kinetic theory [34] of the transport properties of the HS crystal [35, 36]. In this approach, the viscosity tensor of a hard-sphere crystal is expressed in terms of three parts: instantaneous, kinetic, and so called alpha part. The estimation of the last part requires the DFT elastic components.

Acknowledgment

Some of the calculations were performed at the Poznań Supercomputing and Networking Center (PCSS).

References

[1] P. Hohenberg, W. Kohn, *Inhomogeneous Electron Gas*, Physical Review **136**, B864 (1964).

[2] W. Kohn, L.J. Sham, *Self-Consistent Equations Including Exchange and Correlation Effects*, Physical Review **140**, A1133 (1965).

[3] W. Koch, M.C. Holthausen, *A Chemist's Guide to Density Functional Theory*, Wiley (2001).
[4] N.D. Mermin, *Thermal Properties of the Inhomogeneous Electron Gas*, Physical Review **137**, A1441 (1965).
[5] M. Baus, *Statistical mechanical theories of freezing: An overview*, Journal of Statistical Physics **48**, 1129 (1987).
[6] B. Groh, B. Mulder, *Hard-sphere solids near close packing: Testing theories for crystallization*, Physical Review E **61**, 3811 (2000).
[7] Y. Singh, *Density-functional theory of freezing and properties of the ordered phase*, Physics Reports **207**, 351 (1991).
[8] R. McRae, A.D.J. Haymet, *Freezing of polydisperse hard spheres*, The Journal of Chemical Physics **88**, 1114 (1988).
[9] T.V. Ramakrishnan, M. Yussouff, *First-principles order-parameter theory of freezing*, Physical Review B **19**, 2775 (1979).
[10] N. Sushko, P. van der Schoot, M.A.J. Michels, *Density-functional theory of the crystallization of hard polymeric chains*, The Journal of Chemical Physics **115**, 7744 (2001).
[11] J.-P. Hansen, I.R. McDonald, *Theory of Simple Liquids; with Applications to Soft Matter*, Elsevier LTD, Oxford (2013).
[12] P. Tarazona, *A density functional theory of melting*, Molecular Physics **52**, 81 (1984).
[13] M. Baus, J.L. Colot, *Density-Wave Theory of First-Order Freezing in Two Dimensions*, Molecular Physics **55**, 653 (1985).
[14] J.L. Colot, M. Baus, *The freezing of hard spheres*, Molecular Physics **56**, 807 (1985).
[15] R.O. Jones, *Density functional theory: its origins, rise to prominence, and future*, Reviews of Modern Physics **87**, 897 (2015).
[16] H. Löwen, *Density functional theory of inhomogeneous classical fluids: recent developments and new perspectives*, Journal of Physics: Condensed Matter **14**, 11897 (2002).
[17] M. Yussouff, *Generalized structural theory of freezing*, Physical Review B **23**, 5871 (1981).
[18] T.V. Ramakrishnan, *Density-Wave Theory of First-Order Freezing in Two Dimensions*, Physical Review Letters **48**, 541 (1982).
[19] M.V. Jarić, U. Mohanty, *"Martensitic" instability of an icosahedral quasicrystal*, Physical Review Letters **58**, 230 (1987).
[20] G.L. Jones, *Elastic constants in density-functional theory*, Molecular Physics **61**, 455 (1987).
[21] M.V. Jarić, U. Mohanty, *Density-functional theory of elastic moduli: Hard-sphere and Lennard-Jones crystals*, Physical Review B **37**, 4441 (1988).
[22] D. Frenkel, A.J.C. Ladd, *Elastic constants of hard-sphere crystals*, Physical Review Letters **59**, 1169 (1987).
[23] M.V. Jarić, U. Mohanty, *Jarić and Mohanty Reply*, Physical Review Letters **59**, 1170 (1987).
[24] B.B. Laird, J.D. McCoy, A.D.J. Haymet, *Density functional theory of freezing: Analysis of crystal density*, The Journal of Chemical Physics **87**, 5449 (1987).
[25] N. Sushko, P. van der Schoot, M.A.J. Michels, *Density functional theory for the elastic moduli of a model polymeric solid*, The Journal of Chemical Physics **118**, 6594 (2003); Erratum: The Journal of Chemical Physics **119**, 639 (2003).
[26] D.C. Wallace, *Thermodynamics of Crystals*, Dover Publication (1998).
[27] M. Oettel, S. Görig, A. Härtel, H. Löwen, M. Radu, T. Schilling, *Free energies, vacancy concentrations, and density distribution anisotropies in hard-sphere crystals: A combined density functional and simulation study*, Physical Review E **82**, 051404 (2010).
[28] D.A. Young, B.J. Alder, *Studies in molecular dynamics. XIII. Singlet and pair distribution functions for hard-disk and hard-sphere solids*, The Journal of Chemical Physics **60**, 1254 (1974).
[29] K.W. Wojciechowski, K.V. Tretiakov, *Elastic properties of the f.c.c. hard sphere crystal free of defects*, Computational Methods in Science and Technology **8**, 84 (2002).
[30] K.V. Tretiakov, K.W. Wojciechowski, *Poisson's ratio of the fcc hard sphere crystal at high densities*, The Journal of Chemical Physics **123**, 074509 (2005).
[31] S. Pieprzyk, M.N. Bannerman, A.C. Brańka, M. Chudak, D.M. Heyes, *Thermodynamic and dynamical properties of the hard sphere system revisited by molecular dynamics simulation*, Physical Chemistry Chemical Physics **21**, 6886 (2019).
[32] S. Bravo Yuste, A. Santos, *Radial distribution function for hard spheres*, Physical Review A **43**, 5418 (1991).
[33] C.F. Tejero, M. López de Haro, *Direct correlation function of the hard-sphere fluid*, Molecular Physics **105**, 2999 (2007).
[34] H. van Beijeren, M.H. Ernst, *The modified Enskog equation*, Physica **68**, 437 (1973).
[35] J.R. Dorfman, H. van Beijeren, T.R. Kirkpatrick, *Contemporary Kinetic Theory of Matter*, Cambridge University Press (2021).
[36] T.R. Kirkpatrick, S.P. Das, M.H. Ernst, J. Piasecki, *Kinetic theory of transport in a hard sphere crystal*, The Journal of Chemical Physics **92**, 3768 (1990).

Sławomir Pieprzyk is assistant professor at the Institute of Molecular Physics, Polish Academy of Sciences (IMPPAS). He studied Technical Physics at Poznań University of Technology and obtained his PhD in IMPPAS in 2015. His research interests involve computer simulation methods and object-oriented programming, especially for simple liquids and soft matter.

Arkadiusz C. Brańka is professor at the Institute of Molecular Physics, Polish Academy of Science, and studied Physics at the Adam Mickiewicz University in Poznań. He obtained his PhD in ISAS in Trieste in 1986. After his PhD he joined IMPPAS, where in 2002 he received his habilitation degree. His research interests are in the fields of structural, thermodynamics and transport properties of liquids and suspensions, liquid crystals, anomalous elasticity and simulation methods applied to particle systems.

David M. Heyes [PhD, University of Manchester, UK, 1977] has held postdoctoral research positions in the Vitreous State Laboratory, Department of Physics, Catholic University of America, Washington DC, USA, Department of Physical Chemistry at the University of Amsterdam, and at the Department of Chemistry, Royal Holloway, University of London. He was a Royal Society (London) 1983 University Research Fellow between 1983 and 1992, first at Royal Holloway. He is in the Department of Physics, Royal Holloway, University of London, and is a Principal Research Fellow in the Department of Mechanical Engineering, Imperial College London. His current research interests are in the area of the isomorph states of liquids and solids using statistical mechanics theory and molecular simulation, especially where applied to transport coefficients.